Formation of NV centers in diamond: A theoretical study based on calculated transitions and migration of nitrogen and vacancy related defects

Peter Deák,[1,*] Bálint Aradi,[1] Moloud Kaviani,[1] Thomas Frauenheim,[1] and Adam Gali[2,3,†]

[1]*Bremen Center for Computational Materials Science, University of Bremen, PoB 330440, D-28334 Bremen, Germany*

[2]*Wigner Research Center for Physics, Hungarian Academy of Sciences, PoB 49, H-1525 Budapest, Hungary*

[3]*Department of Atomic Physics, Budapest University of Technology and Economics, Budafoki út 8, H-1111 Budapest, Hungary*

(Received 18 September 2013; published 4 February 2014; corrected 21 February 2014)

Formation and excitation energies as well charge transition levels are determined for the substitutional nitrogen (N_s), the vacancy (V), and related point defects (NV, NVH, N_2, N_2V, and V_2) by screened nonlocal hybrid density functional supercell plane wave calculations in bulk diamond. In addition, the activation energy for V and NV diffusion is calculated. We find good agreement between theory and experiment for the previously well-established data and predict missing ones. Based on the calculated properties of these defects, the formation of the negatively charged NV center is studied, because it is a prominent candidate for application in quantum information processing and for nanosensors. Our results indicate that NV defects are predominantly created directly by irradiation, while simultaneously produced vacancies will form V_2 pairs during postirradiation annealing. Divacancies may pin the Fermi level, making the NV defects neutral.

DOI: 10.1103/PhysRevB.89.075203 PACS number(s): 71.15.Mb, 61.72.Bb, 71.55.Ht

I. INTRODUCTION

Diamond has point defects that could act as quantum bits in quantum information processing at room temperature [1,2]. Particularly, the nitrogen-vacancy (NV) defect [3–5] is a prominent candidate, and it can also be used as a nanosensor to detect magnetic [6–11] and electric [12] fields, temperature [13–15], or chemical changes on the surface [16]. All these applications rely on the negative charge state of NV that, however, can also often be found in the neutral charge state in bulk diamond [4,17]. In addition, the negative nitrogen-vacancy, NV(−), may temporarily or permanently lose its charge state during optical excitation [18–21]. The photostability may be improved by postannealing treatments [22].

NV(−) can be routinely found in natural Type Ib diamonds, but generally, the concentration of NV defects in natural or as-grown synthetic diamonds is too low for applications [23]. The concentration of NV defects can be substantially increased by creating vacancies in N-doped diamond by irradiation with energetic neutrons, electrons, or ions [24,25], followed by annealing above ∼600 °C, where vacancies become mobile [4,26]. According to the present consensus in the literature, mobile vacancies are then trapped by substitutional nitrogen (N_s), forming NV centers [27–31].

Understanding the formation of NV defects in as-grown or irradiated diamond samples requires accurate knowledge about the formation energy of the isolated constituents, N_s and the vacancy (V), and about competing defect complexes. The mobility of the species and the energy of complex formation may depend on the charge states; thus, it is highly critical to determine the charge transition levels of these defects across the band gap. Since diamond is a wide gap material, it is extremely difficult (or sometimes impossible) to determine deep adiabatic (thermal) charge transition levels by traditional techniques such as deep-level transient spectroscopy (DLTS). The vertical ionization energies may be obtained by optical excitation of the samples, but it is not trivial to interpret the signals from these experiments. However, recent advances in density functional theory (DFT) have made it possible to calculate transition levels with very good accuracy [32].

In this paper, we apply advanced DFT calculations to determine the formation and excitation energies, the charge transition levels, and the diffusion activation energies for nitrogen- and V-related defects in diamond. We have been able to reproduce the known data with good accuracy and predict the missing ones, which are needed to study the complex formation of these defects in as-grown, as well as irradiated, diamond samples. The effect of extended defects (the surface, grain boundaries, voids, or aggregates) on the formation and charge state of NV is beyond the scope of this paper. We believe that the first step toward following and understanding the atomistic processes of NV creation should inevitable be taken in bulk diamond, considering the simplest and most relevant reaction paths only. Here, we focus our paper particularly on the formation of small complexes, such as the divacancy (V_2), the pair of N_s atoms (N_2), the NV, and the N_2V and NVH centers, from isolated constituents, considering all possible charge states of these defects.

We find that the concentration of NV in as-grown diamond is always at least three orders of magnitude smaller than that of N_s due to the low equilibrium concentration of vacancies. The calculated reaction energies between N_s and V defects indicate that the concentration of NV will not be higher even if a nonequilibrium excess of vacancies are provided due to the preference for V_2 over NV formation. We show, however, that NV formation can be expected to dominate over V formation during irradiation. We also find that V_2 defects crucially influence the charge state of NV and that having the latter predominantly in the negative charge state requires the reduction of the V_2 concentration.

The paper is organized as follows. In Sec. II, the methodology is described in detail. In Sec. III, we provide the results. We analyze each point defect in separate Secs. III A–III G, where we compare our calculations with existing experimental

*Corresponding author: deak@bccms.uni-bremen.de

†Corresponding author: gali.adam@wigner.mta.hu

or theoretical data from previous papers. We discuss the formation and charge state of NV in Sec. III H. Finally, we briefly summarize the results in Sec. IV.

II. METHODS

Defect calculations in solids are almost always carried out by applying two basic approximations: (i) the adiabatic principle, i.e., the separation of the electron problem from that of the lattice vibrations, and (ii) the one-electron approximation, which expresses either the wave function (in Hartree-Fock theory) or the density (in the Kohn-Sham theory) of the many-electron system in terms of independent single-particle states. The neutral vacancy, V(0), in diamond is the schoolbook example for the failure of both of these approximations. Strong electron-phonon coupling gives rise to a dynamic Jahn-Teller effect, obliterating in room-temperature measurements the static Jahn-Teller distortion predicted by theoretical calculations at 0 K, and the degenerate ground state cannot be described with just one single-particle configuration. Still, the system sizes necessary to model V-related defects in the solute limit are just too big for abandoning these approximations. Therefore, they will still be used in this paper in the hope that in calculated energy differences the lack of many-body effects and electron-phonon coupling causes errors of 0.1–0.2 eV at most due to error compensation. As we will show, comparison of our results to experimental data supports this expectation.

Nitrogen- and V-related defects were investigated thoroughly earlier by using DFT within the local density or the generalized gradient approximation (LDA and GGA, respectively) and by semiempirical methods [25,33–38]. While these studies have revealed the basic configurations of the relevant defects, calculated gap levels and optical transitions were impaired even in *ab initio* calculations by the electron self-interaction error involved with the standard approximations of DFT. Precise calculation of these data are important for defect identification, but the correct reproduction of the defect levels is also crucial for calculating relative energies of different configurations and for the activation energy of diffusion [39]. The present calculations have been carried out in the framework of the generalized Kohn-Sham theory [40] by using the screened hybrid functional of Heyd, Scuseria, and Ernzerhof (HSE06) with the original parameters (0.2 $Å^{-1}$ for screening and 25% mixing) [41]. Previously, we have shown [32] that defect levels calculated with this method in group IV semiconductors fulfill the generalized Koopmans' theorem [42]; i.e., the total energy is a linear function of the fractional occupation number. Due to the error compensation between the Hartree-Fock and GGA exchange (which would lead, if applied purely, to concave and convex total energies, respectively), HSE06 in diamond happens to be nearly free of the electron self-interaction error and is capable of providing defect levels and defect-related electronic transitions within ~0.1 eV to experiment [32,43].

We have used the Vienna *Ab initio* Simulation Package (VASP) 5.2.12 with the projector-augmented wave method (applying projectors originally supplied to the 5.2 version) [44]. To avoid size effects as much as possible, a 512-atom supercell was used in the $\mathbf{\Gamma}$ approximation for defect studies. Parameters for the supercell calculations were established first by using the GGA exchange of Perdew, Burke, and Ernzerhof (PBE) [45] in bulk calculations on the primitive cell with a 8 × 8 × 8 Monkhorst-Pack (MP) set for Brillouin-zone sampling [46]. (Increasing the MP set to 12 × 12 × 12 has changed the total energy by <0.002 eV.) Constant volume relaxations using a cutoff of 370 eV in the plane-wave expansion for the wave function and 740 eV in the plane-wave expansion for the charge density resulted in an equilibrium lattice parameter of $a_{\mathrm{PBE}} = 3.570$ Å. Increasing the cutoff to 420 and 840 eV for the wave function and charge density, respectively, has changed the lattice constant by only 0.003 Å. Therefore, considering the demands of the supercell calculations, the lower cutoff was selected. An HSE06 calculation with the 8 × 8 × 8 MP set and 370- and 740-eV cutoff for the wave function and charge density, respectively, resulted in the lattice constant $a_{\mathrm{HSE}} = 3.545$ Å, the bulk modulus $B_0 = 425$ Å, and the indirect band gap $E_g = 5.34$ eV, in good agreement [47] with the experimental values of $a = 3.567$ Å, $B_0 = 443$ GPa, and $E_g = 5.48$ eV (see, e.g., Ref. [39]). Due to the different choice of the basis, the HSE06 values presented here differ somewhat from those in Refs. [32,39,43], but tests on the NV(−) center have shown that the higher cutoff would cause only very small differences in the equilibrium geometry of that defect.

Defects in the supercell were allowed to relax in constant volume until the forces were below 0.01 eV/Å. Diffusion activation energies were determined by the nudged elastic band method (NEB) [48]. For comparison of different defect configurations and charge states, the electrostatic potential alignment and the charge correction scheme of Lany and Zunger was applied [49,50]. In a recent comparative paper on charge corrections [51], the Lany-Zunger scheme [as described there by Eqs. (15) and (20)] was found to work best for defects with medium localization.

Experimental diffusion studies in diamond are performed at high temperatures (800−2200 K), so approximating the free energy of diffusion activation with the energy is quite inaccurate. The strongest temperature-dependent contribution to the free energy in diamond comes from the vibrations. The vibration energy and entropy have been estimated by density-functional-based tight binding (DFTB) [52] calculations, as described earlier for V in silicon carbide [53], using the DFTB+ code [54].

III. RESULTS AND DISCUSSION

A. Substitutional nitrogen

N_s is the most prominent defect of Type Ib natural and N-doped chemical vapor-deposited (CVD) diamond, and it has been thoroughly studied experimentally. It is stable up to high temperatures, with a diffusion activation energy of 5.0 ± 0.3 eV (as measured between 1700 and 2100 °C at a pressure of 7 GPa) [55]. In another high-temperature/high-pressure experiment, a lower barrier of 2.6 eV was found [56], presumably due to the assistance of intrinsic defects generated by pressure effects [55]. Theoretical calculations (at 0 K) find an activation energy of 6.3 eV for the direct exchange of N_s with a neighbor C atom [25], while the rate-limiting step for V-assisted diffusion was found to be the jump

TABLE I. Comparison of the vertical and adiabatic charge transition levels, calculated by HSE06 and experiment. Numbers in parentheses are the estimates with the marker method, based on LDA cluster calculations by Jones *et al*. [60], where available, and the results of a HSE06 calculation by Weber *et al*. [63] in a smaller supercell. Donor levels are given with respect to E_C, and acceptor levels are given with respect to E_V (in electron volts). Detailed geometry of the defects will be provided upon request.

		Vertical		Adiabatic	
Defect	Charge transition level	HSE06 (LDA [60])	Experimental	HSE06 (LDA [60]; HSE06 [63])	Experimental
N_s	(+/0)	$E_C - 3.1$ (2.9)	$E_C - 3.3$[a]	$E_C - 1.8$ (1.5; 1.8)	$E_C - 1.7$[b]
	(0/−)	$E_V + 4.9$ (4.7)		$E_V + 4.6$ (4.4; 4.5)	
V	(2+/+)	$E_C - 5.0$		$E_C - 4.9$	
	(+/0)	$E_C - 4.5$		$E_C - 4.4$ (−; 4.4)	$E_C - 4.3$[c]
	(0/−)	$E_V + 2.1$		$E_V + 2.0$ (−; 1.9)	
	(−/2−)	$E_V + 4.8$		$E_V + 4.9$	
NV	(+/0)	$E_C - 4.6$		$E_C - 4.4$ (−; 4.7)	
	(0/−)	$E_V + 2.7$		$E_V + 2.7$ (−; 2.8)	
	(−/2−)	$E_V + 4.9$		$E_V + 4.9$	
N_2	(+/0)	$E_C - 4.4$		$E_C - 4.0$	$E_C - 4.0$[d]
N_2V	(+/0)	$E_C - 4.8$		$E_C - 4.7$	
	(0/−)	$E_V + 3.3$		$E_V + 3.2$	
V_2	(+/0)	$E_C - 4.3$		$E_C - 4.3$	
	(0/−)	$E_V + 2.4$		$E_V + 2.3$	
	(−/2−)	$E_V + 3.2$		$E_V + 3.2$	
NVH	(+/0)	$E_C - 4.9$		$E_C - 4.5$	
	(0/−)	$E_V + 2.6$		$E_V + 2.4$	$E_V + 2.4$[e]
	(−/2−)	$E_V + 4.6$		$E_V + 4.4$	

[a]Since the excited effective-mass-like states in diamond are within 0.1 eV of the band edges, within the accuracy of the calculations, the vertical ionization energy of N can be compared to the observed *A* band of the optical absorption spectrum (Ref. [57]).
[b]Thermal activation energy of conductivity (Ref. [57]).
[c]DLTS (Refs. [64,65]).
[d]Photoconductivity (Ref. [73]).
[e]Absorption (Ref. [23]).

of N_s into a next-neighbor V, with a calculated barrier of ∼4.8 eV [33,34]. The optical signature of the N_s defect is well known. In ultraviolet absorption the *A* band at 3.3 eV and the *B* band at 3.9 eV were assigned to vertical transitions from the A_1 ground state of the defect to effective-mass-like A_1 and *E* excited states, respectively [57,58]. From the thermal activation of the conductivity, the adiabatic (+/0) charge transition level of N_s was found to be with respect to the conduction band edge (E_C) at $E_C - 1.7$ eV [59]. A negatively charged state of N_s has been predicted theoretically and confirmed experimentally [60,61]. It has been suggested that the zero phonon line (ZPL) measured at 4.059 eV in Type Ib diamonds is associated with the formation of $N_s(-)$ by populating $N_s(0)$ with an additional electron from the valence band. The absorption band at 4.6 eV was assigned to the corresponding vertical transition [57,62]. LDA calculations find N_s to have C_{3v} symmetry, with the distance of N_s to the nearest C neighbor along the trigonal axis being ∼28% longer than the C–C bonds [33]. With the application of the marker method—to correct for the deficiencies of LDA and the cluster model—the vertical (adiabatic) charge transition levels were estimated to be at $E_C - 2.9$ eV ($E_C - 1.5$ eV) for the (+/0) transition and with respect to the valence band edge (E_V) at $E_V + 4.7$ eV ($E_V + 4.4$ eV) for the (0/−) transition [35,60].

Our HSE06 calculation reproduces the C_{3v} symmetry (with one N–C distance elongated by 32%), but also all the experimentally observed electronic transitions with an accuracy better than 0.2 eV and without any *a posteriori* correction. Table I shows the vertical and adiabatic charge transition levels. To check the creation mechanism of $N_s(-)$, we have attempted to calculate an exciton with the electron trapped in the gap level of N_s, but the hole also got localized into a defect-related state above E_V. The vertical excitation energy and the corresponding ZPL for creating such an excited state of N_s are in excellent agreement with the experimental values (Table II). Since nitrogen diffusion without the assistance of

TABLE II. Intradefect vertical transitions and the corresponding ZPL (in electron volts).

		Vertical		ZPL	
Defect	Transition	HSE06	Experimental	HSE06	Experimental
$N_s(0)$	$^1A_1 \rightarrow {}^1A_1$	4.6	4.6[a]	4.1	4.1[a]
V(−)	$^4A_2 \rightarrow {}^4T_1$			3.3	3.3[b]
NV(−)	$^3A_2 \rightarrow {}^3E$	2.3	2.2	2.0	2.0[c]
N_2	$^1A_{1g} \rightarrow {}^1A_u$	4.0		3.6	3.8[d]
$^1N_2V(0)$		2.8		2.7	2.5[e]
$^3N_2V(0)$		2.7		2.6	2.5[e]

[a]References [57,62].
[b]See, e.g., Reference [67].
[c]Reference [4].
[d]Reference [72].
[e]Reference [66].

vacancies only occurs at temperatures and pressures irrelevant for the application of the NV center, we have not attempted to calculate the energy barrier for direct exchange of N_s with a neighboring C atom. V-assisted nitrogen diffusion will be considered in the section about the NV defect.

B. The single V

The single V is the origin of numerous bands in the optical spectra of diamond. The ZPLs of the GR1 band at 1.67 eV and of the ND1 band at 3.15 eV are assigned to the excitation of V(0) and the negative vacancy, V(−), respectively (see, e.g., Ref. [67]). Based on DLTS studies, the adiabatic (+/0) charge transition level was suggested to be at 1.25 or 1.13 eV above the valence band (Ref. [64] or Ref. [65], respectively), corresponding to about $E_C - 4.3$ eV. The (0/−) level is expected to be around midgap [67], which would be hard to detect directly. V(0) is mobile between 600 and 800 °C, with an activation energy of 2.3 ± 0.3 eV, while V(−) is not: the latter probably undergoes a charge transition before diffusing [67].

Theoretically, the unrelaxed V gives rise to a nondegenerate a_1 and a triply degenerate t_2 single-particle defect state, with the latter higher in energy. An $a_1(\uparrow\downarrow)$, $t_2(\uparrow\downarrow{:}0{:}0)$ singlet configuration for V(0) is Jahn-Teller unstable. LDA calculations result in a D_{2d} distortion, with the axial displacement of the first neighbors (parallel to the main symmetry axis) much larger than the radial one [36]. This splits the triply degenerate single-particle state $t_2(\uparrow\downarrow{:}0{:}0)$ into $b_2(\uparrow\downarrow) + e(0{:}0)$. As mentioned in the Methods section, the experimental results on V can be analyzed in terms of many-body states in T_d symmetry [68]. The singlet ^1E ground state of V(0) cannot be described by just one single-particle configuration. The single-particle configuration $a_1(\uparrow\downarrow)$, $b_2(\uparrow\downarrow) + e(0{:}0)$, obtained from LDA calculations, is a weighted sum of the ^1E and the $^1A_1$ many-body states. Performing GGA calculations (with the PBE exchange functional), we could reproduce the D_{2d} state described above for V(0), but we also found a metastable state, 0.24 eV higher in energy, where the axial distortion is smaller than the radial and the splitting of the t_2 single-particle state gives rise to a doubly degenerate e level *lower* in energy than the nondegenerate b_2 state. In the HSE06 calculation, this latter situation turns out to be the ground state. A singlet $a_1(\uparrow\downarrow)$, $e(\uparrow{:}\downarrow) + b_2(0)$ occupation is, in principle, Jahn-Teller unstable, but upon relaxation the geometry nearly preserves the D_{2d} symmetry, with the two spin orbitals, which belong to one given level (after the splitting of $e(\uparrow{:}\downarrow)$ into $b_1(\uparrow) + b_2(\downarrow)$ states), having orthogonal mirror planes. The radial distortion is 12%, and the axial is 5%. This singlet configuration is 0.18 eV lower in energy than a triplet $a_1(\uparrow\downarrow)$, $e(\uparrow{:}\uparrow) + b_2(0)$, with 11% radial and 8% axial distortion. This might well be an artifact of the hybrid functional due to the overestimated strong splitting of the e level [69]. Actually, the triplet $a_1(\uparrow\downarrow)$, $e(\uparrow{:}\uparrow) + b_2(0)$ single-particle configuration is among the degenerate ones that make up the $^3T_1$ excited state of V(0). The latter is known to be 0.1 eV above the singlet ^1E ground state [70]. Since this difference is within the error bar of our calculations, we decided to use the triplet $a_1(\uparrow\downarrow)$, $e(\uparrow{:}\uparrow) + b_2(0)$ single-particle configuration as reference state for V(0). It is reasonable to assume that we are committing the same error when describing V(+) with a single $a_1(\uparrow\downarrow)$, $b_1(\uparrow{:}0) + a_1(0) + b_2(0)$ configuration in C_{2v} symmetry. Indeed, the resulting (+/0) charge transition level (Table I) is within 0.1 eV to the experimental observation. The (0/−) level is predicted at $E_V + 2.0$ eV, i.e., close to midgap, as expected [67].

TABLE III. Diffusion activation energies (in electron volts) from HSE06 (this paper) without and with DFTB corrections for the vibrational energy and entropy at 1000 K, compared to high-temperature experimental data. Numbers in parentheses are from the LDA calculations of Refs. [34,36].

Defect	HSE06 (LDA)	HSE06+DFTB	Experimental
V(0)	2.8 (2.8)	2.6	2.3 ± 0.3[a]
V(−)	3.5 (2.5)		Immobile[a]
NV(0)	4.7 (4.8)	4.5	

[a]Reference [67].

The ground state of V(−) is $^4A_2$ in T_d symmetry, to which only one single-particle configuration is contributing: $a_1(\uparrow\downarrow)$, $t_2(\uparrow{:}\uparrow{:}\uparrow)$, which is stable against static Jahn-Teller distortion [36]. The same is true for the $^4T_1$ excited state of V(−), which is given by the three degenerate $a_1(\uparrow)$, $t_2(\uparrow\downarrow{:}\uparrow{:}\uparrow)$ single-particle configurations. The vertical transition from the ground state to this excited state was calculated to be 3.3 eV with LDA [36], even though a higher energy is expected than the ZPL observed at 3.3 eV. The same calculation resulted in diffusion activation energies of 2.80 and 2.47 eV for V(0) and V(−), respectively, with the saddle point being off the [111] axis in the $(1\bar{1}0)$ plane. While the first value is reasonably close, the second contradicts the experiments, which indicate a much higher activation energy for V(−) [67]. Our HSE06 calculation for V(−) results in 3.3 eV for the ZPL of the ND1 band (Table II), in excellent agreement with experiment. Our results also indicate that V can be stable in 2+ and 2− charge states (Table I). In calculating the diffusion barriers by the NEB method, we have followed the route given in Ref. [36]. While our result for V(0) is identical with that of the LDA calculation (Table III), the HSE06 barrier for V(−) is substantially higher, giving rise to diffusivities 10^6 times smaller than that of V(0) at 1000 K, in agreement with experiment [67]. Taking into account the energy and entropy of vibrations at 1000 K, the calculated free energy of activating the diffusion of V(0) is 2.6 eV, which is within the bounds of the experimental determination, especially when considering the neglect of many body effects.

C. The NV center

The NV(−) color center of diamond is at the focus of many experimental and theoretical papers (see, e.g., Refs. [43,71]). The observed vertical absorption and the ZPL of the NV(−) center can be reproduced well by HSE06 calculations. The values given in Table II differ slightly from our previously published result [43], due to the changes in the parameters of the calculation, but agree well with those of Ref. [63]. We have not calculated the internal transitions of the NV(0) center, because its excited state cannot be described by one single-particle configuration. There are no experimental data available on the charge transition levels. Our calculated

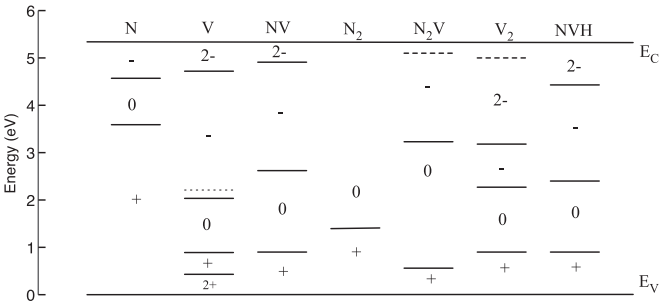

FIG. 1. Comparison of the adiabatic charge transition levels. Dashed lines are estimates based on the vertical ionization energy, computed from the frontier orbitals. The dotted line for the single V arises from an estimate for the singlet many-body ground state (0.1 eV below the first triplet many-body state used for obtaining the solid line).

adiabatic values for the (+/0) and (0/−) levels in Table I are shallower than those of Ref. [63], probably due to the use of the much larger supercell. According to our calculations, an NV(2−) charge state could in principle also exist, but donors shallower than N_s would be needed to obtain them (Fig. 1). Our calculated energy barrier for the jump of the nitrogen atom into V agrees well with the LDA values of Refs. [25,34], but the free energy of activation at high temperature (Table III) is still much higher than the 2.6 eV observed during the aggregation of dispersed N_s into pairs (called *A* aggregate) [56]. Although the latter happens to be close to the activation energy of V(0) diffusion, our result indicates that the aggregation process could not have been assisted by vacancies (leaving only self-interstitials as possible mediators). According to the mechanism proposed in Ref. [34], the N→V jump is also the critical step for the diffusion of the NV center. Our barrier of 4.5 eV indicates that NV centers will remain immobile up to ∼1700 °C, unless self-interstitials (which might assist diffusion) are released from larger aggregates.

D. The N_2 defect

The N_2 defect, i.e., two first-neighbor N_s, was identified as the *A* aggregate in Type IaA diamonds [25,38,72]. It is characterized by a ZPL at 3.8 eV. Such defects can be found only in natural diamonds, or after annealing above 2000 K. It is assumed that the ZPL is connected to a hyperdeep donor level at $E_C - 4.0$ eV [73]. Since this level might influence the charge state of, and is an obvious trap for, vacancies (forming the N_2V center), we have calculated its electronic structure. The ground state is singlet, with just one doubly occupied level in the gap. As shown in Tables I and II, the HSE06 results for the (+/0) charge transition level, as well as the ZPL of the internal excitation of the defect, are in good agreement with experiment. Interestingly, the N_2(+) defect has no occupied level in the gap, so no charge states other than 0 and + can be expected.

E. The N_2V center

NV centers are created by the capture of mobile V(0) at N_s; however, nitrogen clusters are competing traps for the vacancies. The smallest such complex is the *A* aggregate (N_2 or N_s-N_s, see above). By the capture of a V, an N_s-V-N_s complex with C_{2v} symmetry is formed (i.e., V now has two nitrogen and two carbon neighbors) [25,74]. This defect gives rise to the *H*3 optical center, characterized by a ZPL of 2.463 eV due to a transition between the singlet $^1A_1$ and $^1B_1$ states [75]. Time-dependent measurements show also a delayed luminescence with about the same energy from a triplet state, energetically very close to $^1B_1$ [76]. LDA calculations [74] predict that the occupied bonding and the unoccupied antibonding states between the two carbon neighbors to V (at a distance of 2.85 Å from each other) have levels in the gap. The calculated vertical transition energy was found to be 0.93 eV, and the discrepancy with the observed value was attributed to the LDA.

Our (spin-polarized) HSE06 calculation for this complex results in a somewhat larger distance between the carbon neighbors, 2.71 Å, and three levels in the gap. The lowest one is a doubly occupied level 0.1 eV above E_V, and it corresponds to a state weakly localized on the nitrogen neighbors in antibonding combination. The singlet ground state is "antiferromagnetic": the spin-up and spin-down wave functions of the next, occupied gap level are localized on either of the two carbon neighbors. The same is true for the third, unoccupied level. Such ↑ and ↓ states alone do not correspond to the C_{2v} symmetry of the system, yet a relaxation without constraint preserves that symmetry. Apparently the two dangling sp^3 hybrids of the carbon neighbors represent a biradical state that, similarly to the four dangling bonds of the single V, cannot be described with just one single-particle configuration. We have calculated the excitation energies on the assumption that picking just one such configuration for both the ground and the excited states will give a reasonable estimate of the true many-body excitations. For the vertical excitation between the occupied and the unoccupied carbon-related states we have obtained 0.82 eV, close to the LDA prediction. Adiabatic excitation from the lowest gap state (weakly localized to the nitrogen neighbors) to the unoccupied carbon-related state, however, gave reasonably good agreement with the experimentally observed ZPL. We have also found a metastable triplet state that is 0.18 eV above the "antiferromagnetic" singlet ground state. In this case, one electron is on each of the bonding and the antibonding combination of the sp^3 hybrids of the two carbon neighbors. An excited triplet state also exists (with one electron promoted from the antibonding N-N state to the bonding C-C state) that is 0.29 eV higher than the excited singlet state described above. This leads to two recombination channels with similar ZPLs, as measured in experiment [76]. These results show that, despite the limitations due to the single-particle approximation, the HSE06 results are correct on a semiquantitative level. In calculating the charge transition levels, we have taken the antiferromagnetic singlet ground state as reference and expect a similar uncertainty in the values given in Table I as in the case of the single V.

F. The divacancy

When neutral vacancies start to diffuse, divacancies may also form in various charge states. This has to be taken into

account when considering the equilibrium concentration of NV(−) centers. The neutral divacancy, $V_2(0)$, has signatures in both paramagnetic and optical spectra [77,78]. Analysis of the former has led to the surprising conclusion that the ground state of $V_2(0)$ is a triplet in C_{2h} symmetry, instead of the intuitively expected D_{3d} [79]. Coomer *et al.* [37] interpreted this as a result of a level crossing (similar to our case for the single V) due to a strong outward relaxation of those carbon pairs that do not lie in the mirror plane. While this C_{2h} structure was 0.1 eV higher in energy than a D_{3d} one in LDA, it turns out to be the ground state in our HSE06 calculation, being 0.07 eV lower in energy. In the HSE06 ground state, the gap contains only states derived from the e_u and e_g states of the ideal V_2, split up in accordance with the C_{2h} symmetry. Here again, only the sum of the two spin orbitals of the same level transform according to the irreducible representations of the C_{2h} point group, but relaxation without constraint preserves the C_{2h} symmetry. In addition, the lowest-energy singlet and the triplet single-particle configurations have the same energy within the accuracy of the calculation. All this points to a many-body ground state, which cannot be described well in a single-determinant approximation. In our calculations, all vertical excitations between the gap states have lower energy than the ZPL attributed to $V_2(0)$ at 2.543 eV [77]. It appears likely that an a_1 state (still visible in the gap under the D_{3d} symmetry constraint) contributes to the excitation; however, this cannot be taken into account in our one-determinant approximation. The negatively charged divacancy, $V_2(-)$, was proposed as the origin of the W29 paramagnetic center with a quadruplet spin state [80]. We find a quadruplet ground state for $V_2(-)$, supporting this assignment. As shown in Fig. 1, we find the $(-/2-)$ charge transition level of V_2 in the gap, the ground state of $V_2(2-)$ being a triplet. Based on the position of the lowest unoccupied state, even a stable $V_2(3-)$ state appears to be plausible.

G. The NVH center

The NVH center is an important complex in N-doped CVD samples, observed in its negative charge state [23,81]. Theoretical studies [35,82,83] have established that the hydrogen atom binds to one of the carbon neighbors of V in the NV(−) center, dynamically tunneling between the three possible sites and thus exhibiting C_{3v} symmetry in experiments. We have calculated the NVH defect in a static C_{1h} model, as in Ref. [82]. The calculated $(0/-)$ charge transition level nevertheless agrees nicely with the experimental value (Table I).

H. Creation of the NV(−) center

The possibility of manipulating the optical emission and the magnetic states of the NV center makes it a desirable defect for many applications. Therefore, control over the concentration and charge state of this defect is required. However, these depend on the concentration of other defects. Assuming equilibrium conditions, the calculated formation energies allow us to predict the relative concentrations in different charge states by solving the neutrality equation, considering all defects i, with charge q_i:

$$N_C \exp\left[-\frac{E_C - E_F}{kT}\right] + \sum_i |q_i| \cdot (N_{Ai} - p_{Ai}) = N_V \exp\left[-\frac{E_F - E_V}{kT}\right] + \sum_i |q_i| \cdot (N_{Di} - n_{Di}) \quad (1)$$

where

$$N_C = 2\left(\frac{2m_e^* \pi kT}{h^2}\right)^{3/2}; \quad N_V = 2\left(\frac{2m_h^* \pi kT}{h^2}\right)^{3/2} \quad (2)$$

are the effective (number) densities of states in the conduction and valence band of diamond, calculated from the density-of-states mass of the electrons, $m_e^* = 0.57\ m_0$, and the holes, $m_h^* = 0.8\ m_0$, respectively. The remaining terms in Eq. (1) are the occupancies of the acceptor and donor levels, determined by the Fermi-Dirac distribution and the degeneracy factors g

$$p_{Ai} = N_{Ai}\left[g_{Ai}\exp\left(\frac{E_F - E_{Ai}}{kT}\right) + 1\right]^{-1}; \qquad n_{Di} = N_{Di}\left[g_{Di}\exp\left(\frac{E_{Di} - E_F}{kT}\right) + 1\right]^{-1} \quad (3)$$

The defect concentrations in Eq. (1) must be determined from the calculated energies of formation $E_{\text{form}}^{i,q}$ as

$$N_{(A,D)i} = N_{(A,D),i}^0 \exp\left(-E_{\text{form}}^{i,q}/kT\right) \quad (4)$$

for all acceptors (A) and donors (D). Here N_i^0 is the density of i sites in the perfect lattice. We have calculated the defect formation energies with reference to the perfect 512-atom diamond supercell and the chemical potential of nitrogen in the gas phase, μ_N, as

$$E_{\text{form}}^{i,q} = E^q[C_{512} : N_n V_m] - \frac{512 - n - m}{512} E[C_{512}] - n\mu_{\text{N}} + q(E_F + E_V + \Delta V_{\text{align}}) + E_{\text{corr}}^q \quad (5)$$

where E_{corr}^q and ΔV_{align} are the charge and potential alignment corrections, respectively, and E_F is the Fermi energy with respect to E_V. We have chosen μ_N to be half of the HSE06 energy of an N_2 molecule, $E(N_2) = -22.78$ eV, as a reference, to list the calculated formation energies in Table IV. (We also provide the formation energy of the NVH complex, using the energy of a hydrogen atom in a surface C-H bond on the 2×1-reconstructed (001) surface [84], as chemical potential for the hydrogen [85].) Since both Eqs. (1) and (5) contain the Fermi energy, this system of equations has to be solved self-consistently.

In the wide gap insulator diamond, the concept of a Fermi level—as understood in traditional semiconductors—may be of limited use at room temperature (or below) [86], but we consider here the effect of heat treatments ∼1100 K, where it can still be useful to understand the trends of defect formations and their charge states in diamond. Although, NV(−) centers are in practice usually not created in equilibrium processes, the study of scenarios leading to thermal equilibrium will provide insight into the formation process.

First, we study the equilibrium achieved after the heat treatment of N-doped crystals (without prior irradiation), by

TABLE IV. HSE06 formation energies (in electron volts) of the nitrogen- and V-related defects according to Eq. (5), with μ_N = 11.39 eV (corresponding to the energy of a nitrogen atom in the N_2 molecule at 0 K) The formation energies of charged defects are referred to E_V (in Eq. (5)). The chemical potential of hydrogen was set as in Ref. [85] (see text for more details).

Defect	Q	$E^{i,q}_{\text{form}} - qE_F$
N	+	0.37
	0	3.96
	−	8.53
V	2+	5.72
	+	6.15
	0	7.14
	−	9.19
	2−	14.05
NV	+	5.31
	0	6.21
	−	8.82
	2−	13.83
N_2	+	2.55
	0	3.92
N_2V	+	4.78
	0	5.41
	−	8.64
V_2	+	9.08
	0	10.08
	−	12.42
	2−	15.59
NVH	+	4.34
	0	5.19
	−	7.59
	2−	12.19

assuming different nitrogen concentrations. It is known from the study of type Ib natural diamonds that nitrogen impurities do not aggregate when the concentration of nitrogen is below 500 ppm, unless the temperature is above 2000 K. Therefore, one can exclude the formation of N_2 and N_2V defects in a heat treatment at lower temperature. In practice, the nitrogen concentration depends on the growth conditions (temperature, pressure, and nitrogen precursors present), which determine the chemical potential of nitrogen. Here we tune the value of μ_N (and with it the values in Table IV) in order to set the total concentration of nitrogen defects in the desired region between 10 and 500 ppm. We solved Eqs. (1)–(5) self-consistently under these conditions, assuming the formation of N_s, V, NV, and V_2 defects in a heat treatment at the example temperature of T = 1100 K. We find that V and V_2 practically do not form because of their much too high formation energies. As shown in Fig. 2(a), the calculated $[N_s]/[NV]$ concentration ratio is constantly $\sim 10^3$ under these conditions; in other words, [NV] is 0.1% of $[N_s]$. As a consequence, the Fermi level is pinned at $E_V + 4.0$ eV, and the vast majority of N_s are neutral; only ∼0.3% will be positively and 0.2% will be negatively charged. Thus, ∼0.1% of the N_s defects donates an electron to NV defects. As a consequence, all the NV defects will be negatively charged. All in all, our calculations indicate that NV(−) is introduced at concentrations < 1 ppm in lightly N-doped diamond, where neutral N_s (with s = 1/2 electron spin) will dominate the sample. Our simulation assumes infinite bulk diamond, so we do not consider surface band bending, which can convert NV(−) to NV(0) [87].

Next, we consider higher nitrogen contents between 1000 and 3000 ppm, which correspond to Type Ia natural diamonds. In this case, the average distance between nitrogen impurities is just a few lattice constants; thus, nitrogen impurities may aggregate even at a relatively low temperature such as 1100 K, and N_2 and N_2V may form under these conditions. To simulate these conditions, we tuned μ_N to set the total concentration of nitrogen defects in the desired region and considered all the defects in all charge states as listed in Table IV, except NVH. Our simulations indicate [Fig. 2(b)] that nitrogen occurs predominantly as $N_2(0)$, while a small fraction of N_s and N_2V (∼1 ppb) can coexist. The NV concentration is negligible under these conditions. Since N_2 stays in the neutral charge state, the Fermi level is pinned near the acceptor level of N_2V at $\sim E_V + 3.2$ eV, so the neutral charge state of that defect is slightly more abundant than the negative one.

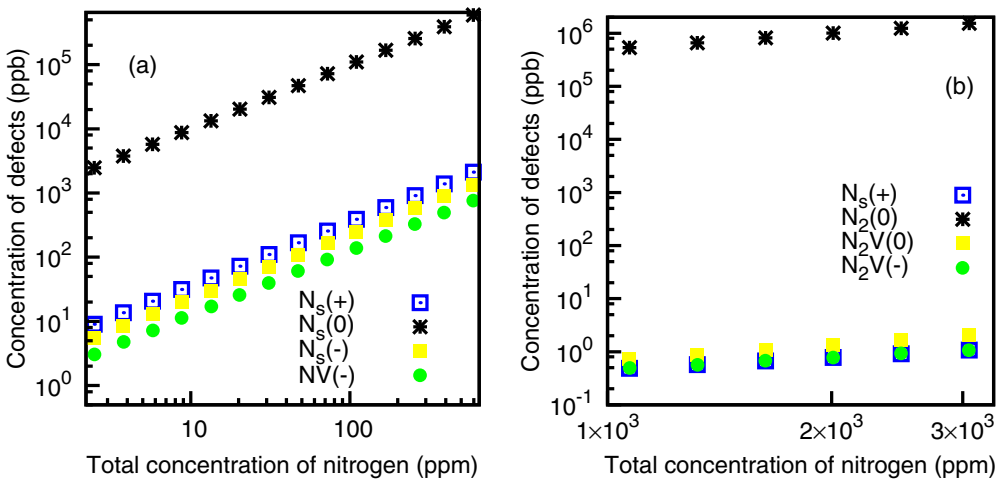

FIG. 2. (Color online) Calculated concentrations of defects characteristic in (a) Type Ib and (b) Type IaA diamonds after annealing at 1100 K. The other defects with the corresponding charge states have lower concentrations and not shown in these plots.

Synthetic diamonds can also be grown by CVD, with substrate temperatures ~1100 K. Here, the formation of NV is influenced by hydrogen impurities, which enter the crystal in the CVD process. According to recent experiments, NVH defects (see Sec. III G) form in a ratio of 0.01–0.02 to the incorporated N_s, when the concentration of N_s is ~0.5–1.2 ppm [23,81,88]. The concentration of NV is below the detection limit of 0.1 ppb in these samples, which means $[NV]/[N_s] < 0.1\%$. According to the calculated formation energies (Table IV), the NVH complex has ~1 eV lower formation energy than that of NV. This result explains why the NVH defect can outcompete the NV defect in a CVD diamond. The NVH complex is stable against annealing up to 1600 °C [23,89]. Above that temperature, NV defects can already diffuse; thus, NVH defects cannot be converted to NV by thermal annealing. So, the NV concentration in CVD samples is again insufficient for practical applications.

In practice, the concentration of NV(−) centers can be increased by irradiation and subsequent annealing. The irradiation creates Frenkel pairs (and other damage) in the diamond lattice. Annealing leads to recombination, but some Frenkel pairs may split to produce isolated vacancies and self-interstitials with concentrations much above that of thermal equilibrium. The self-interstitials are mobile even at room temperature; they will aggregate to the surface or grain boundaries or form plateletlike defects. In the meantime, they can assist nitrogen diffusion and aggregation. Subsequent to irradiation, a heat treatment has to be applied to anneal out luminescence-quenching parasitic defects. This is usually done slightly above 600 °C, where neutral vacancies become mobile. It is usually assumed that NV centers are formed during this heat treatment when vacancies get trapped at N_s defects. However, vacancies may also get trapped at existing N_2 defects or can form divacancies. The postirradiation annealing can be regarded as a quasiequilibrium process, and an insight into the creation of NV(−) centers can be gained by close inspection of the formation energies and occupation levels of the considered defects. First, one can assume that the initial concentration of isolated N_s defects is high enough to pin the Fermi level initially above the midgap. In order to have mobile, i.e., neutral vacancies after the irradiation, the Fermi level must be lowered drastically, below the single acceptor level of V ($\sim E_V + 2.0$ eV). Thus, if NV defects are to be created by irradiation and annealing, the V concentration should be in excess of the N_s concentration ($[V] > [N_s]$), even after the trivial recombination with interstitials. Then, two basic reactions can occur:

$$V(0) + V(0) \rightarrow V_2(0) + 4.2\ \text{eV} \quad (6)$$

and

$$V(0) + N_s(+) \rightarrow NV(0) + h + 3.3\ \text{eV}, \quad (7)$$

where h is a hole with energy corresponding to the given Fermi-level position. Both reactions are strongly exothermic, as can be derived from the data in Table IV [90]. Since $[V] > [N_s]$ and Eq. (6) provides a higher energy gain than Eq. (7), the majority of the vacancies will form divacancies; only a small fraction creates NV defects. Since the formation of V_2 is ~0.9 eV more favorable than that of NV, the equilibrium concentration of V_2 will be several orders of magnitude larger than that of NV, even at relatively high temperatures (at 1100 K by a factor of 2×10^4). This implies that the concentration of NV defects, arising through the reaction in Eq. (7), will not be significantly higher than they would be without irradiation. In addition, the generally assumed process of creating NV defects by V diffusion would be self-limiting. As isolated vacancies start to form V_2 and NV defects, the Fermi level shifts up, because both V_2 and NV are deeper acceptors than V (cf. Fig. 1). As a result, the remaining isolated vacancies will become negatively charged and immobilized. So increasing the V concentration cannot help to increase [NV].

The observed increase in [NV] can, therefore, be explained only by assuming that NV defects dominantly form during irradiation, not during the annealing. Our results support this assumption. With the data of Table IV, the creation of a V near N_s requires an energy of

$$N_s(0) + 2.26\ \text{eV} \rightarrow NV(0) + C, \quad (8)$$

while that of a V in a perfect part of the crystal needs

$$\text{perfect lattice} + 7.14\ \text{eV} \rightarrow V(0) + C, \quad (9)$$

where C is a carbon atom in the perfect diamond lattice. The reason for the difference is that to remove the C atom opposite to N_s requires us to break only three strong C-C bonds (see Sec. III A), whereas four such bonds have to be broken in the perfect diamond lattice to form an isolated V. Such a big energy difference should lead to a strong preference for NV creation even in the nonequilibrium process of irradiation, explaining most of the arising NV concentration. We conclude, therefore, that the dominant part of the NV concentration is created directly by the irradiation.

According to our simplified model, the dominant point defects in N-doped, irradiated, and annealed diamond samples are N_s, NV, and V_2. The charge state of the NV defect will depend on the relative concentrations of the N_s donors and the V_2 acceptors. To study the chances for creating negatively charged NV centers, we have tuned the formation energies of these three defects to obtain a total nitrogen concentration of 386 ppm and an N_s-to-NV conversion factor of 1.4% (i.e., within the range of experimental observations between 0.5 and 2.5%), at various $[V_2]/[N_s]$ ratios. Figure 3 shows how the $[NV(-)]/[NV(0)]$ ratio depends on $[V_2]/[N_s]$.

If divacancies dominate, i.e., $[V_2]/[N_s] > 1$, then the Fermi level will be pinned near the single acceptor level of V_2 at $E_V + 2.3$ eV. Since the first acceptor level of NV is at $E_V + 2.7$ eV, our simulation results in an $[NV(-)]/[NV(0)]$ concentration ratio of ~0.1. Therefore, for $[V_2] > [N_s]$ the neutral NV would dominate. Reducing $[V_2]$ will shift the Fermi level toward the acceptor level of NV and, as soon as $[V_2]/[N_s] < 1$, the negative charge state of NV becomes dominant. Our simulation demonstrates (Fig. 3) that the charge state of NV is very sensitive to the concentration of V_2 in this range. Changing the concentration of V_2 by less than a factor of two, can change the $[NV(-)]/[NV(0)]$ ratio by a factor of ~100.

These results show that the postirradiation annealing not only does not contribute significantly to the NV production but also, by creating divacancies, may prevent the achievement of negatively charged NV defects. The annealing is unavoidable, but our analysis indicates that its temperature should be chosen

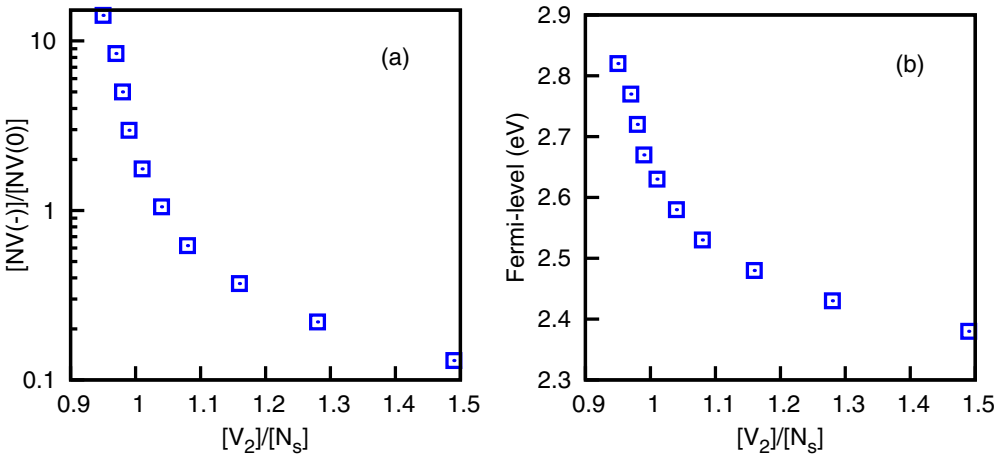

FIG. 3. (Color online) (a) The calculated concentration ratio [NV(−)]/[NV(0)] and (b) the corresponding Fermi-level position (with respect to E_V) as a function of the ratio of $[V_2]/[N_s]$ at $T = 1100$ K. The total concentration of nitrogen is set to ∼386 ppm, while the N_s-to-NV conversion factor is 1.4%.

in the range where V_2 becomes mobile while NV does not. This is possible as the TH5 center, associated with V_2, starts to anneal out from 800 °C [78,91], where NV is not yet mobile. (We emphasize here that annealing out $V_2(0)$ defects can raise the Fermi level, which will change the charge state of the residual V_2 from neutral to negative. Thus, the $V_2(-)$ signals should be monitored, as well as $V_2(0)$, to determine the concentration of the remaining divacancies at elevated temperatures.)

The annihilation of the divacancies may occur by outdiffusion but also by recombination at interstital clusters or by the formation of V aggregates, which are also electrically active [92–95]. However, it appears likely that the V aggregates are acceptor defects, with a charge transition level $\sim E_V + 3.5$ eV [23]. This is well above the (0/−) level of NV, so they can donate electrons to turn NV(0) to NV(−). Thus, elimination of V_2 can stabilize the charge state of NV(−).

Our analysis is in line with the observed higher efficiency of NV(−) creation, when annealing irradiated diamonds at higher than usual temperatures (1100–1200 °C) [31]. The annihilation of V_2 is important even when $[NV(-)]/[NV(0)] > 1$ happens to be the case after irradiation and annealing, because V_2 will be negatively charged under this condition and can compromise the photostability of NV(−). High-temperature postannealing treatments could help stabilize the charge state of NV(−) [22]. Our results highlight the need for careful characterization of irradiated and annealed diamond samples, particularly focusing on V_2 or larger V aggregates [96], and the need for more detailed studies of the annealing temperature.

IV. SUMMARY AND CONCLUSIONS

We calculated the charge transition levels, excitation energies, barrier energy for migration, and reaction energies of basic V- and nitrogen-related defects by the HSE06 supercell plane wave method. We have reproduced the known experimental data regarding electronic transitions, substantially improving over previous (standard) DFT calculations. In particular, without any *a posteriori* correction, our HSE06 calculation reproduces *all* experimentally observed charge transition levels and internal transitions within 0.2 eV. In contrast to standard DFT, we find that the relaxation of the atoms around a V(0) (larger in the radial than in the axial direction of D_{2d}) splits the doubly occupied t_2 single-particle state into a lower-lying e state and a higher-lying b_2 state. A spin-triplet occupation of the e state realizes the $^3T_1$ excited many-particle state, which is known to lie 0.1 eV above the ^1E ground state. Taking that into account, the position of the (+/0) charge transition level (the only one known experimentally) is reproduced within 0.1 eV. Unlike standard DFT, HSE06 correctly finds the symmetry of the neutral-, and the spin state of the negative vacancy. Our calculations also provide the first explanation for the observed luminescence of N_2V, reproducing the observed transition energies within 0.2 eV in both the singlet and the triplet recombination channels. The proven accuracy of the method has allowed us to predict missing data on the charge transitions of all the investigated defects (N_s, V, NV, NVH, N_2, N_2V, and V_2), which are crucial for establishing the charge state of different defects. Our results also comply with the experimental finding on the migration of isolated V, i.e., that only its neutral form is mobile, while it is immobile in its negative charge state.

By assuming quasiequilibrium conditions, we found that the NV center may be created in lightly N-doped diamond ($[N] < 500$ ppm) in small concentration, whereas the formation of N_2V defects is more likely for high concentrations ($[N] > 1000$ ppm). We also investigated the basic reaction for the formation of NV centers in irradiated and annealed samples. The key findings are that

(i) Irradiation is more likely to directly create NV defects than vacancies.

(ii) In postirradiation annealing, much more divacancies are formed than NV defects, and only short-range diffusion of vacancies toward proximate N_s defects can increase the concentration of NV centers.

(iii) Since V_2 is a deeper acceptor than NV, the created NV defects will dominantly be in the neutral charge state, unless the concentration of divacancies is sufficiently decreased by annealing above ∼1100 K.

(iv) Remaining divacancies may influence the photostability of NV(−) centers.

ACKNOWLEDGMENTS

A.G. gracefully acknowledges through support grants from the Seventh Framework Programme of the European Commission for the Diamond Based Atomic Nanotechnologies, and Diamond Devices Enabled Metrology and Sensing, projects. A.G. also acknowledges support from the MTA Lendület program (Hungarian Academy of Sciences). The support of the North-German Supercomputing Alliance (Grant No. 0011) is appreciated. Fruitful discussions with J. Wrachtrup are also appreciated.

[1] L. Childress, M. V. Gurudev Dutt, J. M. Taylor, A. S. Zibrov, F. Jelezko, J. Wrachtrup, P. R. Hemmer, and M. D. Lukin, Science **314**, 281 (2006).
[2] S.-Y. Lee, M. Widmann, T. Rendler, M. W. Doherty, T. M. Babinec, S. Yang, M. Eyer, P. Siyushev, B. J. M. Hausmann, M. Loncar, Z. Bodrog, A. Gali, N. B. Manson, H. Fedder, and J. Wrachtrup, Nat. Nanotechnol. **8**, 487 (2013).
[3] L. du Preez, Ph.D. thesis, University of Witwatersrand, Johannesburg, RSA, 1965.
[4] G. Davies and M. F. Hamer, Proc. R. Soc. A **348**, 285 (1976).
[5] J. H. N. Loubser and J. P. van Wyk, in *Diamond Research (London)* (Industrial Diamond Information Bureau, London, UK, 1977), p. 11.
[6] J. R. Maze, P. L. Stanwix, J. S. Hodges, S. Hong, J. M. Taylor, P. Cappellaro, L. Jiang, M. V. Gurudev Dutt, E. Togan, A. S. Zibrov, A. Yacoby, R. L. Walsworth, and M. D. Lukin, Nature **455**, 644 (2008).
[7] G. Balasubramanian, I. Y. Chan, R. Kolesov, M. Al-Hmoud, J. Tisler, Ch. Shin, Ch. Kim, A. Wojcik, P. R. Hemmer, A. Krueger, T. Hanke, A. Leitenstorfer, R. Bratschitsch, F. Jelezko, and J. Wrachtrup, Nature **455**, 648 (2008).
[8] H. J. Mamin, M. Kim, M. H. Sherwood, C. T. Rettner, K. Ohno, D. D. Awschalom, and D. Rugar, Science **339**, 557 (2013).
[9] T. Staudacher, F. Shi, S. Pezzagna, J. Meijer, J. Du, C. A. Meriles, F. Reinhard, and J. Wrachtrup, Science **339**, 561 (2013).
[10] M. S. Grinolds, S. Hong, P. Maletinsky, L. Luan, M. D. Lukin, R. L. Walsworth, and A. Yacoby, Nat. Phys. **9**, 215 (2013).
[11] D. Le Sage, K. Arai, D. R. Glenn, S. J. DeVience, L. M. Pham, L. Rahn-Lee, M. D. Lukin, A. Yacoby, A. Komeili, and R. L. Walsworth, Nature **496**, 486 (2013).
[12] F. Dolde, H. Fedder, M. W. Doherty, T. Nöbauer, F. Rempp, G. Balasubramanian, T. Wolf, F. Reinhard, L. C. L. Hollenberg, F. Jelezkoand, and J. Wrachtrup, Nat. Phys. **7**, 459 (2011).
[13] G. Kucsko, P. C. Maurer, N. Y. Yao, M. Kubo, H. J. Noh, P. K. Lo, H. Park, and M. D. Lukin, Nature **500**, 54 (2013).
[14] D. M. Toyli, C. F. de las Casas, D. J. Christle, V. V. Dobrovitski, and D. D. Awschalom, Proc. Natl. Acad. Sci. USA **110**, 8417 (2013).
[15] P. Neumann, I. Jakobi, F. Dolde, C. Burk, R. Reuter, G. Waldherr, J. Honert, T. Wolf, A. Brunner, J. H. Shim, D. Suter, H. Sumiya, J. Isoya, and J. Wrachtrup, Nano Lett. **13**, 2738 (2013).
[16] V. Petráková, A. Taylor, I. Kratochvilová, F. Fendrych, J. Vacik, J. Kučka, J. Štursa, P. Cígler, M. Ledvina, A. Fišerová, P. Kneppo, and M. Nesládek, Adv. Funct. Mater. **22**, 812 (2012).
[17] Y. Mita, Phys. Rev. B **53**, 11360 (1996).
[18] R. U. A. Khan, P. M. Martineau, B. L. Cann, M. E. Newton, and D. J. Twitchen, J. Phys. Condens. Matter **21**, 364214 (2009).
[19] G. Waldherr, J. Beck, M. Steiner, P. Neumann, A. Gali, Th. Frauenheim, F. Jelezko, and J. Wrachtrup, Phys. Rev. Lett. **106**, 157601 (2011).
[20] K. Beha, A. Batalov, N. B. Manson, R. Bratschitsch, and A. Leitenstorfer, Phys. Rev. Lett. **109**, 097404 (2012).
[21] P. Siyushev, H. Pinto, M. Vörös, A. Gali, F. Jelezko, and J. Wrachtrup, Phys. Rev. Lett. **110**, 167402 (2013).
[22] B. Naydenov, F. Reinhard, A. Lämmle, V. Richter, R. Kalish, U. F. S. D'Haenens-Johansson, M. Newton, F. Jelezko, and J. Wrachtrup, Appl. Phys. Lett. **97**, 242511 (2010).
[23] R. U. A. Khan, B. L. Cann, P. M. Martineau, J. Samartseva, J. J. P. Freth, S. J. Sibley, C. B. Hartland, M. E. Newton, H. K. Dhillon, and D. J. Twitchen, J. Phys. Condens. Matter **25**, 275801 (2013).
[24] F. Waldermann, P. Olivero, J. Nunn, K. Surmacz, Z. Wang, D. Jaksch, R. Taylor, I. Walmsley, M. Draganski, P. Reichart, A. D. Greentree, D. N. Jamieson, and S. Prawer, Diam. Relat. Mater. **16**, 1887 (2007).
[25] A. Mainwood, Phys. Rev. B **49**, 7934 (1994).
[26] A. T. Collins and I. J. Kiflawi, J. Phys. Condens. Matter **21**, 364209 (2009).
[27] G. Davies, Nature **269**, 498 (1977).
[28] J. R. Rabeau, P. Reichart, G. Tamanyan, D. N. Jamieson, S. Prawer, F. Jelezko, T. Gaebel, I. Popa, M. Domhan, and J. Wrachtrup, Appl. Phys. Lett. **88**, 023113 (2006).
[29] S. Pezzagna, B. Naydenov, F. Jelezko, J. Wrachtrup, and J. Meijer, New J. Phys. **12**, 065017 (2010).
[30] J. O. Orwa, C. Santori, K.-M. C. Fu, B. Gibson, D. Simpson, I. Aharonovich, A. Stacey, A. Cimmino, P. Balog, M. Markham, D. Twitchen, A. D. Greentree, R. G. Beausoleil, and S. Prawer, J. Appl. Phys. **109**, 083530 (2011).
[31] V. M. Acosta, E. Bauch, M. P. Ledbetter, C. Santori, K.-M. C. Fu, P. E. Barclay, R. G. Beausoleil, H. Linget, J. F. Roch, F. Treussart, S. Chemerisov, W. Gawlik, and D. Budker, Phys. Rev. B **80**, 115202 (2009).
[32] P. Deák, B. Aradi, T. Frauenheim, E. Janzén, and A. Gali, Phys. Rev. B **81**, 153203 (2010).
[33] E. B. Lombardi, A. Mainwood, K. Osuch, and E. C. Reynhardt, J. Phys. Condens. Matter **15**, 3135 (2003).
[34] H. Pinto, R. Jones, D. W. Palmer, J. P. Goss, P. R. Briddon, and S. Öberg, Phys. Status Solidi B **209**, 1765 (2012).
[35] J. P. Goss, P. R. Briddon, R. Jones, and S. Sque, Diam. Relat. Mater. **13**, 684 (2004).
[36] S. J. Breuer and P. R. Briddon, Phys. Rev. B **51**, 6984 (1995).
[37] B. J. Coomer, A. Resende, J. P. Goss, R. Jones, S. Öberg, and P. R. Briddon, Phys. B **273**(2), 520 (1999).
[38] R. Jones, P. R. Briddon, and S. Öberg, Philos. Mag. Lett. **66**, 67 (1992).
[39] P. Deák, B. Aradi, A. Gali, and T. Frauenheim, Phys. Status Solidi B **248**, 790 (2011).

[40] F. Fuchs, J. Furthmüller, F. Bechstedt, M. Shishkin, and G. Kresse, Phys. Rev. B **76**, 115109 (2007).

[41] J. Heyd, G. E. Scuseria, and M. Ernzerhof, J. Chem. Phys. **118**, 8207 (2003); J. A. V. Krukau, O. A. Vydrov, A. F. Izmaylov, and G. E. Scuseria, *ibid.* **125**, 224106 (2006).

[42] S. Lany and A. Zunger, Phys. Rev. B **80**, 085202 (2009).

[43] A. Gali, E. Janzén, P. Deák, G. Kresse, and E. Kaxiras, Phys. Rev. Lett. **103**, 186404 (2009).

[44] G. Kresse and J. Hafner, Phys. Rev. B **49**, 14251 (1994); G. Kresse and J. Furthmüller, *ibid.* **54**, 11169 (1996); G. Kresse and D. Joubert, *ibid.* **59**, 1758 (1999).

[45] J. P. Perdew, K. Burke, and M. Ernzerhof, Phys. Rev. Lett. **77**, 3865 (1996).

[46] H. J. Monkhorst and J. K. Pack, Phys. Rev. B **13**, 5188 (1976).

[47] Our calculated gap does not contain any correction for electron-phonon interaction. It is reasonable to suppose, though, that defect-to-band transitions are influenced by the electron-phonon interaction in approximately the same manner.

[48] G. Mills, H. Jónsson, and G. K. Schenter, Surf. Sci. **324**, 305 (1995).

[49] S. Lany and A. Zunger, Phys. Rev. B **78**, 235104 (2008).

[50] S. Lany and A. Zunger, Phys. Rev. B **81**, 113201 (2010).

[51] H.-P. Komsa, T. T. Rantala, and A. Pasquarello, Phys. Rev. B **86**, 045112 (2012).

[52] Th. Frauenheim, G. Seifert, M. Elstner, Z. Hajnal, G. Jungnickel, D. Porezag, S. Suhai, and R. Scholz, Phys. Status Solidi B **217**, 41 (2000).

[53] E. Rauls, T. Frauenheim, A. Gali, and P. Deák, Phys. Rev. B **68**, 155208 (2003).

[54] B. Aradi, B. Hourahine, and Th. Frauenheim, J. Phys. Chem. A **111**, 5678 (2007).

[55] T. Evans and Z. Qi, Proc. R. Soc. A **381**, 159 (1982).

[56] R. M. Chrenko, R. E. Tuft, and H. M. Strong, Nat. Lett. **270**, 141 (1977).

[57] J. Koppitz, O. F. Schirmer, and M. Seal, J. Phys. C **19**, 1123 (1986).

[58] W. J. P. van Enckevort and E. H. Versteegen, J. Phys. Condens. Matter **4**, 2361 (1992).

[59] R. G. Farrer, Solid State Commun. **7**, 685 (1969).

[60] R. Jones, J. P. Goss, and P. R. Briddon, Phys. Rev. B **80**, 033205 (2009).

[61] R. Ulbricht, S. T. van der Post, J. P. Goss, P. R. Briddon, R. Jones, R. U. A. Khan, and M. Bonn, Phys. Rev. B **84**, 165202 (2011).

[62] M. H. V. Nazaré and A. J. Neves, J. Phys. C **20**, 2713 (1987).

[63] J. R. Weber, W. F. Koehl, J. B. Varley, A. Janotti, B. B. Buckley, C. G. Van de Walle, and D. D. Awschalom, Proc. Natl. Acad. Sci. USA **107**, 8513 (2010).

[64] C. E. Nebel, R. Zeisel, and M. Stutzmann, Diam. Relat. Mater. **10**, 639 (2001).

[65] P. Murret, J. Pernot, T. Teraji, and T. Ito, Phys. Status Solidi A **205**, 2179 (2008).

[66] J. A. van Wyk and G. S. Woods, J. Phys. Condens. Matter **7**, 5901 (1995).

[67] G. Davies, S. C. Lawson, A. T. Collins, A. Mainwood, and S. J. Sharp, Phys. Rev. B **46**, 13157 (1992).

[68] J. E. Lowther, Phys. Rev. B **48**, 11592 (1993).

[69] The splitting of the e level is an artifact of the single-particle approximation. In a multideterminant treatment, one would have to combine the single-determinant electron configurations $e(\uparrow{:}\downarrow)$ and $e(\downarrow{:}\uparrow)$ to describe the true many-body state. The single-determinant Kohn-Sham description, however, artificially picks one of the two configurations. In addition, the orbital-dependent hybrid functional splits the e level, yielding the biradicallike configuration $b_1(\uparrow)b_2(\downarrow)$. This electron configuration, however, is not compatible with the D_{2d} point group symmetry of the nuclei but rather exhibits artificial symmetry lowering of the electronic system to the C_{2v} symmetry.

[70] M. Heidari Saani, M. A. Vesaghi, K. Esfarjani, T. Ghods Elahi, M. Saiari, H. Hashemi, and N. Gorjizadeh, Phys. Rev. B **71**, 035202 (2005).

[71] A. Gali, M. Fyta, and E. Kaxiras, Phys. Rev. B **77**, 155206 (2008).

[72] G. Davies, J. Phys. C **9**, L537 (1976).

[73] E. Rohrer, C. F. O. Graeff, R. Janssen, C. E. Nebel, M. Stutzmann, H. Güttler, and R. Zachai, Phys. Rev. B **54**, 7874 (1996).

[74] R. Jones, V. J. B. Torres, P. R. Briddon, and S. Öberg, Mater. Sci. Forum **143–147**, 45 (1994).

[75] G. Davies, M. H. Nazaré, and M. F. Hamer, Proc. R. Soc. A **351**, 245 (1976).

[76] E. Pereira and T. Monteiro, J. Luminesc. **48-49**, 814 (1991).

[77] M. A. Lea-Wilson, J. N. Lomer, and J. A. van Wyk, Philos. Mag. B **72**, 81 (1995).

[78] C. D. Clark, R. W. Ditchburn, and H. B. Dyer, Proc. R. Soc. A **237**, 75 (1956).

[79] D. J. Twitchen, M. E. Newton, J. M. Baker, T. R. Anthony, and W. F. Banholzer, Phys. Rev. B **59**, 12900 (1999).

[80] J. K. Kirui, J. A. van Wyk, and M. J. R. Hoch, Diam. Relat. Mater. **8**, 1569 (1999).

[81] C. Glover, M. E. Newton, P. Martineau, D. J. Twitchen, and J. M. Baker, Phys. Rev. Lett. **90**, 185507 (2003).

[82] J. P. Goss, P. R. Briddon, R. Jones, and S. Sque, J. Phys. Condens. Matter **15**, S2903 (2003).

[83] M. J. Shaw, P. R. Briddon, J. P. Goss, M. J. Rayson, A. Kerridge, A. H. Harker, and A. M. Stoneham, Phys. Rev. Lett. **95**, 105502 (2005).

[84] Calculated in 22-layer slab model.

[85] T. Miyazaki, H. Okushi, and T. Uda, Phys. Rev. Lett. **88**, 066402 (2002).

[86] A. T. Collins, J. Phys. Condens. Matter **14**, 3743 (2002).

[87] B. Grotz, M. V. Hauf, M. Dankerl, B. Naydenov, S. Pezzagna, J. Meijer, F. Jelezko, J. Wrachtrup, M. Stutzmann, F. Reinhard, and J. A. Garrido, Nat. Comm. **3**, 729 (2012).

[88] R. C. Cruddace, M. E. Newton, H. E. Smith, G. Davies, D. Fisher, P. M. Martineau, and D. J. Twitchen, in *58th De Beers Diamond Conference* (Coventry, UK, 2007), p. 19.1.

[89] B. L. Cann, Ph.D. thesis, University of Warwick, Coventry, UK, 2009.

[90] The capture of a V by N_2 to form N_2V is even more exothermic than Eqs. (6) and (7), so all existing N_2 complexes will likely be turned into N_2V. Still, we assume that the concentration of N_2 defects created during the outdiffusion of self-interstitials is relatively low with respect to $[N_s]$.

[91] K. Iakoubovskii and A. Stesmans, J. Phys. Condens. Matter **14**, R467 (2002).

[92] J. N. Lomer and A. M. A. Wild, Radiat. Eff. **17**, 37 (1973).

[93] G. Davies, *Properties and Growth of Diamond* (INSPEC, London, UK, 1994), Chap. 5.

[94] K. Iakoubovskii and A. Stesmans, Phys. Rev. B **66**, 045406 (2002).

[95] L. S. Hounsome, R. Jones, P. M. Martineau, M. J. Shaw, P. R. Briddon, S. Öberg, A. T. Blumenau, and N. Fujita, Phys. Status Solidi A **202**, 2182 (2005).

[96] T. Yamamoto, T. Umeda, K. Watanabe, S. Onoda, M. L. Markham, D. J. Twitchen, B. Naydenov, L. P. McGuinness, T. Teraji, S. Koizumi, F. Dolde, H. Fedder, J. Honert, J. Wrachtrup, T. Ohshima, F. Jelezko, and J. Isoya, Phys. Rev. B **88**, 075206 (2013).